ACS OMEGA

http://pubs.acs.org/journal/acsodf

Article

Curcumin-Loaded Bioactive Polymer Composite Film of PVA/Gelatin/Tannic Acid Downregulates the Pro-inflammatory Cytokines to Expedite Healing of Full-Thickness Wounds

Nida Rashid, Syed Haroon Khalid, Ikram Ullah Khan, Zunera Chauhdary, Hira Mahmood, Ayesha Saleem, Muhammad Umair, and Sajid Asghar*

Cite This: *ACS Omega* 2023, 8, 7575−7586

Read Online

ACCESS | Metrics & More | Article Recommendations | Supporting Information

ABSTRACT: Curcumin (Cur) entrapped poly(vinyl alcohol) (PVA)/gelatin composite films were prepared by cross-linking with tannic acid (TA) as bioactive dressings for rapid wound closure. Films were evaluated for mechanical strength, swelling index, water vapor transmission rate (WVTR), film solubility, and *in-vitro* drug release studies. SEM revealed uniform and smooth surfaces of blank (PG9) and Cur-loaded composite films (PGC4). PGC4 exhibited excellent mechanical strength (tensile strength (TS) and Young's modulus (YM) were 32.83 and 0.55 MPa, respectively), swelling ability (600−800% at pH 5.4, 7.4, and 9), WVTR (2003 ± 26), and film solubility (27.06 ± 2.0). Sustained release (81%) of the encapsulated payload was also observed for 72 h. The antioxidant activity determined by DPPH free radical scavenging showed that the PGC4 possessed strong % inhibition. The PGC4 formulation displayed higher antibacterial potential against *S. aureus* (14.55 mm zone of inhibition) and *E. coli* (13.00 mm zone of inhibition) compared to blank and positive control by the agar well diffusion method. An *in-vivo* wound healing study was carried out on rats using a full-thickness excisional wound model. Wounds treated with PGC4 showed very rapid healing about 93% in just 10 days post wounding as compared to 82.75% by Cur cream and 80.90% by PG9. Furthermore, histopathological studies showed ordered collagen deposition and angiogenesis along with fibroblast formation. PGC4 also exerted a strong anti-inflammatory effect by downregulating the expression of pro-inflammatory cytokines (TNF-α and IL-6 were lowered by 76% and 68% as compared to the untreated group, respectively). Therefore, Cur-loaded composite films can be an ideal delivery system for effective wound healing.

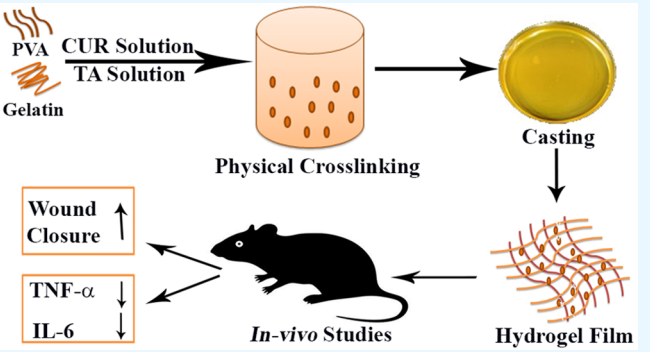

1. INTRODUCTION

In healthcare systems, full-thickness wounds are a considerable clinical challenge. Minor skin injuries may heal rapidly, while full-thickness wounds are susceptible to microbial attack that delays the healing process. Therefore, when the skin is damaged, instant covering with an appropriate dressing is necessary to avoid wound complications and to promote skin healing. Currently, various conventional dressings like natural or synthetic bandages, gauzes, and lint have been used for wound treatment, but they are unable to maintain a damp environment at the wound site, are permeable to microbes, and adhere to the wound leading to secondary injury.[1]

Nowadays, novel strategies for wound care are developed by fabrication of modern wound dressings like biopolymer-based hydrogel films with antimicrobial, antioxidant, and anti-inflammatory properties. Biopolymer-based hydrogel films, having 3D interpenetrating cross-linked networks, are composed of hydrophilic polymers. These hydrogel films are capable for effective wound healing due to their biocompatibility, biodegradable nature, nontoxicity, suitable water vapor transmission rate (WVTR), and antimicrobial potential, and they also maintain a moist environment at the wound site.[2] A single polymer cannot offer all the favorable features of a wound dressing. Mostly natural polymers are preferred due to their biodegradability and biocompatibility to human skin, while synthetic polymers have effective mechanical strength, thermal stability, and less swelling and are toxic in nature.[3] Composites of natural polymers such as oxidized cellulose derivatives with synthetic polymers have also been developed to control bleeding during surgeries.[4]

Gelatin is a natural complex biological macromolecule obtained from collagen denaturation.[5] It has found many

Received: October 31, 2022
Accepted: February 3, 2023
Published: February 20, 2023

applications in tissue engineering owing to its cell adhesion and wound healing properties, biodegradability, biocompatibility, water holding capacity, and film forming ability.[6,7] As reported earlier, the film forming ability and stimulation of new tissue growth by this polymer would offer a better choice in the preparation of wound dressing material.[8] Thus, gelatin is mostly preferred in scaffold preparation, used for tissue rejuvenation and wound contraction.[9] However, easy degradation and low mechanical strength are the main drawbacks of gelatin that could be overcome by blending with other polymers.

Poly(vinyl alcohol) (PVA) is a nontoxic synthetic polymer with high tensile strength.[10] In biomedical sciences, PVA has numerous applications due to its biocompatibility, high hydrophilicity and film forming ability.[11] Therefore, it has been widely used for wound dressing material.[12] PVA could be cross-linked with other synthetic or natural polymers to prepare hydrogels.[13] Tannic acid (TA), $C_{76}H_{52}O_{46}$, is a gallic ester of D-glucose extracted from plants and microorganisms.[14] TA not only acts as a functional agent but can also cross-link various polymers. It has the ability to make molecular complexes with biological macromolecules like carbohydrates and proteins.[15] TA has antimicrobial and antioxidant potential due to its polyphenolic groups. Moreover, TA is widely used in food and medical applications, as it is an FDA approved excipient.[16]

Curcumin (Cur, 1,7-bis(4-hydroxy-3-methoxyphenyl)-1,6-heptadiene-3,5-dione) is a bioactive polyphenolic natural hydrophobic compound extracted from *Curcuma longa*. For effective wound healing, Cur's potential is mostly attributed to its antimicrobial, antioxidant, and anti-inflammatory properties, but its low solubility and poor dissolution profile offer major challenges. Recently, Cur-loaded PVA-TA cryogels were reported to display appropriate antimicrobial and antioxidant potential.[17] Free radical species observed at wound site are the substantial cause of inflammation during the healing process. Cur inhibits the reactive oxygen (ROS) and nitrogen species formation by its anti-inflammatory potential and hence rapidly reduces the inflammation at the wound site.[18,19] It is apparent that Cur's wound healing potential can be optimized by designing a suitable delivery vehicle. Cur incorporation in a polymeric matrix would be a suitable way to control its release for maximum therapeutic activity. Therefore, in this work, PVA/gelatin-based Cur-loaded composite films were prepared by physical cross-linking with the bioactive TA. The physicochemical characteristics of the composite films, *in vitro* performance, and *in vivo* wound healing efficiency were tested to establish this composite film as a wound dressing.

2. MATERIALS AND METHODS

2.1. Materials. Cur (MW = 368.39 g/mol, CAS Number 458-37-7) was purchased from Spectrum Chemical Mfg. Corp. (USA). Gelatin type A (CAS Number 9000-70-8), Tween 80 (CAS Number 9005-65-6), and glycerol were purchased from Daejung (Korea). PVA (CAS Number 9002-89-5), TA, and 2,2-diphenyl-1-picrylhydrazyl (DPPH) were purchased from Sigma-Aldrich (USA). All other chemical reagents used were of analytical grade.

2.2. Preparation of Polymeric Composite Film. Biopolymer-based composite films were prepared by the already reported solvent casting method with some modifications.[20] Aqueous solutions of PVA (1.25%) and gelatin (3.75%) were prepared separately in distilled water under constant stirring (500 rpm) at 90 and 25 °C, respectively, until both polymers were entirely dissolved and clear liquid solutions were attained. The PVA solution was kept cooling at 25 °C; later, the gelatin solution was added slowly in the PVA solution under constant stirring. Meanwhile, 1 mL of an ethanolic solution of 1−2% Cur (w/w based on the mass of polymers) with Tween 80 (0.6%) was added drop by drop to the polymeric solution at constant stirring (700 rpm) for 15 min at room temperature. Then, glycerol (25% w/w based on the mass of polymers) was added to the polymeric mixture to enhance the plasticity of the film. Afterward, 1 mL of TA aqueous solution (0.625% w/w based on the mass of polymers) was added dropwise into the final polymeric solution and continuously stirred until the solution became homogeneous. The resultant homogeneous solution was transferred to a Petri dish and dried at room temperature. Films were peeled off after drying from Petri plates and stored in desiccators.

2.3. Physical Characterization. The thicknesses of the polymeric composite films at different sites were measured through a digital micrometer (Shang Chong Co. Ltd., China) with 0.001 mm precision.[21] Weight uniformity of the films was assessed by taking five random samples (n = 5) (1 × 1 cm^2), and the weight of each sample was calculated individually through an electronic weighing balance (OHAUS adventurer Analytical balance, USA).[22] The folding endurance of the hydrogel films was determined manually by folding the films at the same point for many times, and the number of times a film could be folded without any crack or breaking was noted as the value of folding strength of each film sample.[23] The results of all parameters were reported as mean ± SD.

2.4. Entrapment Efficiency. The entrapment efficiencies of Cur-loaded hydrogel films were determined by placing preweighed samples of definite area (2 × 2 cm^2) in 10 mL of solvent (mixture of ethanol and freshly prepared pH 7.4 phosphate buffer USP (30:70)) for 48 h at 37 °C. Then, polymeric debris was removed by centrifuging the whole solution, and the clear supernatant solution was analyzed by using a UV−visible spectrophotometer (Cecil instrument, Cambridge, England) at 423.5 nm. Values were taken in triplicate and recorded as mean ± SD.[24]

$$\%\ \text{Drug entrapment efficiency} = \frac{\text{Actual drug content}}{\text{Theoretical drug content}} \times 100$$

2.5. Swelling Index. The swelling indexes of polymeric composite films (blank and drug loaded) were recorded by immersing preweighed film specimens of fixed dimension (1 × 1 cm^2) in buffer solutions of different pH (5.4, 7.4, and 9) at room temperature. Films were taken out from buffer solution at different time intervals, and the weight of the swollen film was noted after blotting with filter paper.[2] Three samples (n = 3) from each film were used, and swelling was determined by the following formula:

$$\text{Swelling}\ (\%) = \frac{W_t - W_i}{W_i} \times 100$$

W_t states the weight at a specified time interval, and W_i refers to the initial weight of the dry film.

2.6. Mechanical Evaluation, Water Solubility, Water Vapor Transmission Rate (WVTR). The mechanical testing of composite film samples (tensile strength and young modulus) was evaluated by a DMA analyzer (Q800, TA Instruments; USA) at 25 °C. Polymeric films were cut by using a double blade cutter into strips of typical dimensions of 20 mm × 6 mm. Tensile strength (TS) and Young's modulus (YM)

https://doi.org/10.1021/acsomega.2c07018
ACS Omega 2023, 8, 7575−7586

were assessed by TA Universal Analysis software.[25] The following formula was used to calculate TS:

$$\text{Tensile strength (MPa)} = \frac{\text{Force}}{\text{Area}}$$

Each sample was analyzed in triplicate ($n = 3$), and mean values were stated.

The water solubility of films was evaluated by dissolved dry matter in water after soaking as reported elsewhere.[26] Film samples of suitable dimensions (2×2 cm^2) were dried at 40 °C for 24 h, and the initial dry weight (Wi) of films was determined. The films were soaked in 30 mL of distilled water for 24 h with agitation occasionally, and samples were taken out at filter paper from water and again redried for 24 h at 40 °C. Undissolved, redried film pieces were weighed (W_f).[27] The experiment was carried out for three different samples from each film, and the film solubility was determined by the following equation:

$$\text{Water Solubility (\%)} = \frac{W_i - W_f}{W_i} \times 100$$

WVTR values of composite film samples were assessed to determine moisture permeability. Films trimmed out into circular shape with a specific diameter of 15 mm were affixed over the top of a dry glass vials having 5 g of $CaCl_2$ as desiccant, which were then sealed with tape (water resistant) to prevent the loss of moisture from the edges. Afterward, the vials were weighed accurately and kept in a humidity chamber at constant temperature and humidity for 24 h. WVTR was computed by the given equation:

$$\text{WVTR} \left(\frac{\text{g/m}^2}{\text{day}}\right) = \frac{W}{S} \times 100$$

Here, W refers to desiccant weight gain, and S refers to exposed film area (m^2).[22]

2.7. Solid State Characterization. *2.7.1. Fourier Transform Infrared Spectroscopy (FT-IR).* FTIR analyses were carried out by using IRTracer-100 FTIR (Shimadzu, Japan), and 32 scans were captured for each spectrum in a scanning array of 4000−400 cm^{-1} wave numbers with resolution of 4 cm^{-1}.[28]

2.7.2. X-ray Diffractometric Analysis (XRD). All specimens were assessed by X-ray diffractometer (X'pert PRO, PANalytical, Netherlands) with Cu Kα radiation source. Data were collected over a scanning range of 0−40° (2θ) operated at 30 mA current with a 40 kV voltage.[29]

2.7.3. Scanning Electron Microscopy (SEM). Scanning electron microscopy (VEGA3 TESCAN equipped with four lens) was used to assess the surface view at 20 kV accelerating voltage.[30]

2.8. *In-Vitro* Drug Release Study. The *in-vitro* drug release patterns of Cur encapsulated composite films were investigated by a Franz diffusion cell (Laboratory enterprises, India). A receptor compartment having a capacity of 9 mL was filled with dissolution media (mixture of methanol + PBS 7.4 pH (30:70 ratio)). A cellulose acetate membrane (25 mm) was used as supportive membrane, completely equilibrated with PBS pH 7.4 and placed between both compartments.[31] Films of 15 mm diameter were placed over the membrane surface and remained in contact with the receptor media. The release profile of Cur was attained at different time intervals over a period of 72 h by sampling a 0.5 mL aliquot from the receptor media. The receptor media was replenished with same volume of fresh media each time after sampling. Then a UV−visible spectrophotometer (Cecil instrument, Cambridge, England) was used to analyze each aliquot at 432.5 nm against a methanol−water mixture (30:70 ratio) as blank. The cumulative amount of drug release was calculated by using a previously made calibration curve and plotted against time. Experiments were performed in triplicate ($n = 3$).[32] Cur release kinetics from composite films were analyzed by fitting the release data in the Korsmeyer−Peppas equation, that is given below:

$$M_t / M_\infty = Kt^n$$

From this equation, M_t represents the Cur release amount at time t, while M_∞ refers to the drug release amount at infinite time. K and n are a kinetic constant and the release exponent, respectively.

2.9. Biological Evaluation. *2.9.1. Antibacterial Activity.* The antimicrobial potentials of the blank and Cur loaded composite films were checked by the previously stated agar well method with some modifications[19] against *S. aureus* (Gram-positive) and *E. coli* (Gram-negative) bacteria, as these bacteria colonize within 48 h around the injury. In this method, circular discs of polymeric composite films of 9 mm diameter and nutrient agar medium were both sterilized at 121 °C for 20 min. Nutrient agar medium was poured into sterile plastic plates and solidified. Then, about 100 μL of inoculum comprising almost 10^6−10^7 CFU/mL of tested bacteria was streaked over the media. Wells were made with sterilized borer in Petri plates, and test samples of the films were placed into the wells under sterilized conditions and kept in an incubator for 48 h at 37 °C. After incubation, the antibacterial effect was examined by determining the zone of inhibition all-round the films.

2.9.2. In-Vitro Antioxidant Activity. The radical scavenging potential of Cur-loaded composite films was observed by 2,2-diphenyl-1-picrylhydrazyl radical (DPPH) with slight modification of a previously described method. Briefly, 1.5 mL portions of Cur solutions (5, 10, 25, 50, 100, and 150 μg/mL) were added to 0.5 mL of DPPH solution (0.2 mM methanolic solution), while DPPH (0.2 mM) solution in methanol was used as control. About 100 mg of film specimen was vortexed in 5 mL of a methanol and water (1:1) mixture for 5 min and placed for 24 h at 37 °C in a shaking water bath to dissolve it completely. Afterward, from the film solutions, 1.5 mL of different aliquots equivalent to the above tested free Cur were added in 0.5 mL of DPPH solution. Then, the mixture was thoroughly stirred and incubated in the dark for 30 min at room temperature. The absorbances of the mixtures were determined at 517 nm by a UV−visible spectrophotometer (Cecil instrument, Cambridge, England).[33] All experiments were repeated in triplicate ($n = 3$). The free radical scavenging potential by DPPH of all samples was assessed by the given formula:

$$\text{Free radical scavenging activity (\%)} = \frac{A_c - A_s}{A_c} \times 100$$

where A_c states the absorbance of DPPH, while A_s is the absorbance of the test samples.

2.9.3. In-Vivo Wound Healing Study. An *in-vivo* animal study was conducted by a full thickness excisional wound model in albino rats, and all experimental protocols were authorized by the institutional Ethical Review Committee (ERC) of Govern-

https://doi.org/10.1021/acsomega.2c07018
ACS Omega 2023, 8, 7575−7586

Table 1. Screening of Components of Composite Films for Optimum Physical Characteristics

Formulations	PVA (%w/v)	Gelatin (%w/v)	TA (%w/w)	Cur (%w/w)	Thickness (mm)	Weight uniformity (g)	Folding endurance	EE %
PG1	1.25	2.5			0.141 ± 0.003	0.023 ± 0.001	159 ± 5	
PG2	1.25	3.75			0.161 ± 0.001	0.030 ± 0.003	163 ± 5	
PG3	2.5	1.25			0.110 ± 0.001	0.018 ± 0.001	125 ± 7	
PG4	3.75	1.25			0.125 ± 0.003	0.020 ± 0.002	117 ± 5	
PG5	1.25	2.5	0.3125		0.158 ± 0.004	0.023 ± 0.003	195 ± 7	
PG6	1.25	2.5	0.625		0.162 ± 0.003	0.023 ± 0.002	193 ± 9	
PG7	1.25	2.5	1.25		0.169 ± 0.002	0.023 ± 0.001	205 ± 7	
PG8	1.25	3.75	0.3125		0.199 ± 0.001	0.031 ± 0.002	204 ± 14	
PG9	1.25	3.75	0.625		0.204 ± 0.001	0.031 ± 0.002	206 ± 7	
PG10	1.25	3.75	1.25		0.211 ± 0.002	0.034 ± 0.002	194 ± 9	
PGC1	1.25	3.75		1	0.203 ± 0.002	0.032 ± 0.002	152 ± 7	95.00 ± 1.92
PGC2	1.25	3.75		1.5	0.205 ± 0.003	0.032 ± 0.003	149 ± 5	92.34 ± 1.86
PGC3	1.25	3.75		2	0.207 ± 0.001	0.035 ± 0.001	151 ± 5	77.32 ± 1.19[a,b]
PGC4	1.25	3.75	0.625	1	0.207 ± 0.003	0.034 ± 0.001	206 ± 7	89.40 ± 1.13[a,c]
PGC5	1.25	3.75	0.625	1.5	0.212 ± 0.002	0.035 ± 0.003	215 ± 9	86.49 ± 1.81[a,b,c]
PGC6	1.25	3.75	0.625	2	0.217 ± 0.002	0.0038 ± 0.003	209 ± 6	66.61 ± 2.89[a,b,c,d,e]

[a]Iindicates significant difference ($p < 0.05$) compared to PGC1. [b]Indicates significant difference ($p < 0.05$) compared to PGC2. [c]Indicates significant difference ($p < 0.05$) compared to PGC3. [d]Indicates significant difference ($p < 0.05$) compared to PGC4. [e]Indicates significant difference ($p < 0.05$) compared to PGC5.

ment College University Faisalabad, Pakistan (ref. No: GCUF/ERC/28). In this study, all acquired animals were acclimatized under standard laboratory conditions for 1 week at relative humidity (55 ± 5%), constant temperature (22 ± 2 °C), and 12 h of light/dark cycle along with free access to water and diet.

First, rats were anesthetized with intraperitoneal injection (ketamine + xylazine); then fur was shaved on the dorsal side, and skin was cleansed by using 70% ethyl alcohol throughout the infliction of the experimental wound. Afterward, two 5 mm diameter full thickness wounds were excised by using a biopsy punch. Wounded animals were classified into four groups having three rats ($n = 3$) in each group. Group (i) negative control animals received only sterile normal saline, group (ii) rats served as positive control (disease group), group (iii) animals received Cur cream topically, and group (iv) and (v) rats were treated by blank (PG9) and Cur-loaded composite film (PGC4), respectively. Cur cream was made as reported in the literature[34] for comparative evaluation. Composite films were changed regularly, and wound dimensions were measured with digital calipers at the zeroth, second, fourth, sixth, eighth, and 10th day to find the percentage wound closure (WC) by using the formula given below.

$$\text{Wound closure (\%)} = \frac{A_0 - A_t}{A_0} \times 100$$

where A_0 represents the initial wound area at day zero and A_t refers to the wound area at a specific day.[35]

2.9.4. Histopathological Examination. The skin samples of rats were taken on the 10th day of experiment after euthanasia. For histopathological investigation, tissue samples were fixed in 10% formalin buffered solution followed by alcoholic dehydration and embedded in paraffin tissue blocks. Demonstrative sections were stained with H&E and Masson's Trichrome, and photomicrographs of each section were examined under an Accu-scope 3000-LED microscope.[18]

2.9.5. Assessment of Inflammatory Biomarkers. Pro-inflammatory cytokines (interleukin-6 (IL-6) and tumor necrosis factor-α (TNFα)) in the serum of rats were investigated by ELISA kits (Elabscience, Wuhan, China) according to the manufacturer's procedure. Each sample was analyzed in triplicate ($n = 3$), and the optical density values of each sample were verified by using the standard curve.[33]

2.10. Statistical Analysis. All experiments were repeated in triplicate ($n = 3$), and data were expressed as mean ± standard deviation. A nonparametric two-tailed student's t test or one-way ANOVA was used for statistical comparison. $p < 0.05$ indicated a statistically significant difference.

3. RESULTS AND DISCUSSION

3.1. Preformulation and Physical Evaluation of Composite Films. Composite films prepared from gelatin alone were brittle in nature. Therefore, a blend of PVA and gelatin cross-linked by TA was used in different ratios and concentrations as shown in Table 1.

The thickness and weight of composite films ranged from 0.110 to 0.217 mm and 0.018 to 0.038 g, respectively, depending upon the overall solid content of films.[36] Overall, the composite films displayed lower degree of variability in weight and thickness. Folding endurance, the capability of composite films to resist against any rupture, varied from 117 to 215. Folding endurance was greater for films containing higher gelatin proportion, whereas addition of TA increased the folding endurance of films due to cross-linking of the polymeric chains mediated by hydrogen bonding as depicted in Figure 2A, which remained almost the same even upon encapsulation of the Cur. Results indicate adequate mechanical strength of films with sufficient elasticity required for the handling and application of the wound dressings.[37]

TA concentration was optimized on the basis of physical integrity and swelling in PBS 7.4 pH. As shown in Figure S1, as the concentration of TA increased, the swelling decreased but the films remained intact for 72 h when cross-linked with 0.625% and 1.25% TA, whereas films cross-linked with 0.3125% TA could not preserve their integrity beyond 24 h, as these turned into gel lumps due to maximum hydration. Films containing higher gelatin ratio showed maximum swelling due to their higher hydration capacity. In addition to the film integrity, swelling is a significant parameter for a wound

https://doi.org/10.1021/acsomega.2c07018
ACS Omega 2023, 8, 7575−7586

dressing for controlled release of drug and for exudate sponging. Hence, PG9 was considered for drug loading.

3.2. Entrapment Efficiency (EE%). EE% values of composite films were evaluated to quantify the total amount of drug entrapped into the film matrix as shown in Table 1. To solubilize Cur, ethanol was used as cosolvent and Tween 80 as surfactant for the uniform distribution of drug in the film matrix with homogeneous film structure.[38] The average percentage of drug entrapment ranged from 77% to 95% for non-cross-linked films, whereas it was 66% to 89% for cross-linked preparations depending upon the amount of drug loading. Increasing the drug content decreased the EE%, and a significantly lower EE% was observed for the 2% Cur-loaded film. In addition, cross-linking hampered the loading of drug within the matrix of the film, and this effect was more pronounced for the 2% Cur loading film (PGC6). Cross-linking could have resulted in a tighter and more compact 3D hydrogel network, thus reducing the capacity of the films to load the drug. Hence, the 1% Cur-loaded film (PGC4) revealed higher incorporation of Cur with minimal drug loss and was selected for further experiments.

3.3. Swelling Ratio. The swelling ability and the magnitude of swelling act as a rate-determining step for release of drug and absorption of exudate at the wound site from a hydrogel-based wound dressing.[39] The pH of intact skin is 5.4, and it changes continually during the wound alleviation process.[40] So, the swelling capabilities of composite films were characterized at different pH. The swelling degrees of PG9, PGC1, and PGC4 films are summarized in Figure 1. Swelling of PG9 and PGC4

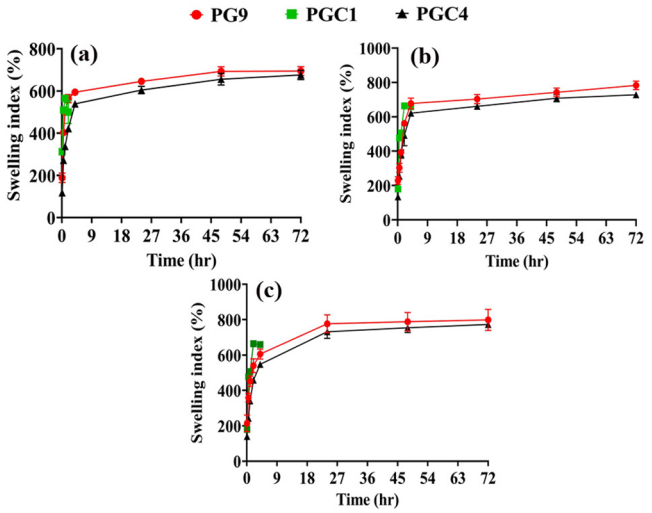

Figure 1. Swelling indexes of composite films in (a) pH 5.4 buffer, (b) pH 7.4 buffer, and (c) pH 9 buffer. Error bars indicate standard deviation (n = 3).

was maintained up to 72 h. The mechanism of polymer swelling in aqueous media can be described by two different ways: First, the increase in film affinity for water was due to the water solubility of gelatin and its high amount in the film matrix, so water ingression into the matrix caused the film matrix to swell.[41] Second, swelling may also occur due to repulsion among the adjacent amines in gelatin that become positively charged in water and could have raised the swelling ratio.[42]

3.4. Mechanical Properties, Water Solubility, and Water Vapor Transmission Rate (WVTR). The mechanical properties of composite films rely on intermolecular interactions in polymer chains and fillers' distribution.[43] The tensile strength (TS) and Young's modulus (YM) are the parameters of a wound dressing that reveal the mechanical properties during use[6] as depicted in Figure 2B.

The TS and YM of the blank film (PG9) were 30.20 and 0.59 MPa, respectively. Acosta et al. reported identical mechanical properties for a starch/gelatin blend.[44] The TS of PGC4 (Cur-loaded formulation) increased nonsignificantly (32.83 MPa, $p > 0.05$), as the even distribution of Cur in the film matrix could make productive stress transfer at the film interface.[36] A nonsignificant decrease in YM (0.55 MPa, $p > 0.05$) due to Cur loading was also noted, as the hydrophobicity of Cur might have influenced the degree of cross-linking of the protein.[45]

Film water solubility is one of the important parameters of effective wound dressing to determine film integrity. The film solubilities of different formulations are shown in Figure 2B. Film solubility primarily depends upon the nature and concentration of additives, along with the hydrophilic–hydrophobic index.[46] Film solubility increases upon incorporation of hydrophilic compounds, whereas it decreases in the presence of cross-linkers and incorporation of hydrophobic compounds.[47] PGC4 displayed statistically insignificant ($p > 0.05$) reduction in water solubility (27.06%) as compared to PG9 (37.09%), which can be attributed to the hydrophobic nature of Cur. The reduced water solubility of PGC4 is a valuable characteristic for retaining the film's integrity upon exposure to the liquid exudate of wounds.

Optimum WVTR is a key property for an ideal wound dressing to impede dehydration and accretion of exudates at the wound area. Gelatin and PVA are hydrophilic polymers, so they can engross more water vapors, but cross-linking of gelatin chains would decrease it significantly,[48] as cross-linking reduces the free spaces within the polymeric matrix and causes a dense film structure, which resists diffusion of water molecules leading to lower WVTR.[49] As shown in Figure 2B, the WVTR of PG9 (2052 ± 9.7) was slightly higher ($p > 0.05$) compared to that of PGC4 (2003 ± 26.4) having hydrophobic content. The permissible range of WVTR for an ideal dressing ranges from 2000 to 2500 g/m^2/day to avoid dehydration and for appropriate wound care.[50] Hence, the Cur-loaded composite film fabricated in this study would preserve a moist environment at the injured site to accelerate healing.

3.5. Solid-State Characterization. *3.5.1. FTIR Analysis.* FTIR analysis was used to identify the different functional groups and to explore any chemical interaction between drug and other excipients of films. The FTIR spectra of pure Cur, PVA, gelatin, TA, PG9, and PGC4 are depicted in Figure 2C. Pure Cur revealed absorption bands at 3510 and 1627.97 cm^{-1} indicating the presence of a phenolic group and amide I linkages, respectively, and the peaks at 1602 and 1510 cm^{-1} were accredited to symmetric aromatic ring C═C and also mixed C═C and C═O stretching vibrations, respectively.[21] The absorption peak at 1279 cm^{-1} was accredited to C—O stretching, and the peaks observed at 953 cm^{-1}, 806 cm^{-1}, and 713 cm^{-1} represented the C—H bending of the alkene group.[51]

FTIR analysis of PVA showed characteristic bands at 3450 and 2930 cm^{-1} due to the O—H and aliphatic C—H stretching vibrations, respectively. The absorption bands at 1735 and 1579 cm^{-1} were assigned to the C—O stretching from the carboxylic acid and acetate groups, respectively. The peaks at 1112 and 1013 cm^{-1} have been accredited to the C—O and C═OH stretching vibration, respectively.[6,52] Furthermore, the FTIR spectrum of neat gelatin exhibited absorption bands at about 3410 cm^{-1}, 2932 cm^{-1}, 1650 cm^{-1}, and 1535 cm^{-1},

https://doi.org/10.1021/acsomega.2c07018
ACS Omega 2023, 8, 7575−7586

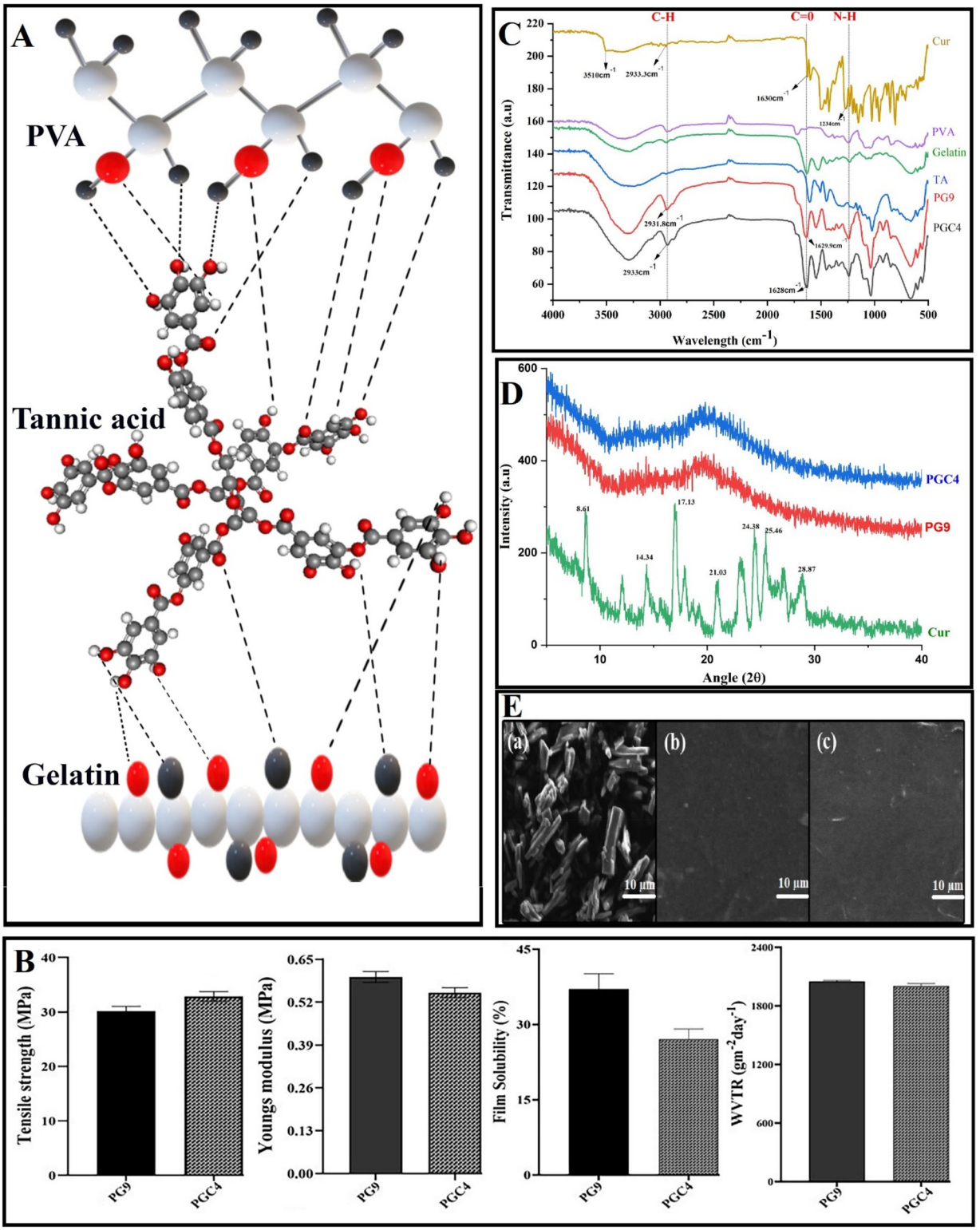

Figure 2. (A) Cross-linking scheme of polymers via hydrogen-bonding provided by TA in the composite film (TA structure obtained from https://molview.org). (B) Tensile strength, Young's modulus, water solubility, and WVTR of optimized blank and drug-loaded films. (C) FTIR spectra of pure Cur, PVA, G, TA, PG9, and PGC4 obtained by ATR-FTIR. (D) XRD patterns of pure Cur, PG9, and PGC4 revealing the solid-state of the samples. (E) SEM micrographs of the surface view of (a) pure Cur, (b) PG9, and (c) PGC4.

corresponding to the stretching vibrations of NH and OH, C—H, and C—O and the bending vibrations of N—H, respectively. Moreover, in TA's spectrum, a distinctive absorption band at 3700−3100 cm^{-1} was assigned to the stretching vibration of various phenolic groups. The peaks observed at 1700 and 1612 cm^{-1} were accredited to the ester C═O and C═C aromatic bond stretchings, respectively. The C—O and aryl oxygen stretchings were seen at 1310 and 1083 cm^{-1}, respectively, while the bending vibrations of OH and the

https://doi.org/10.1021/acsomega.2c07018
ACS Omega 2023, 8, 7575−7586

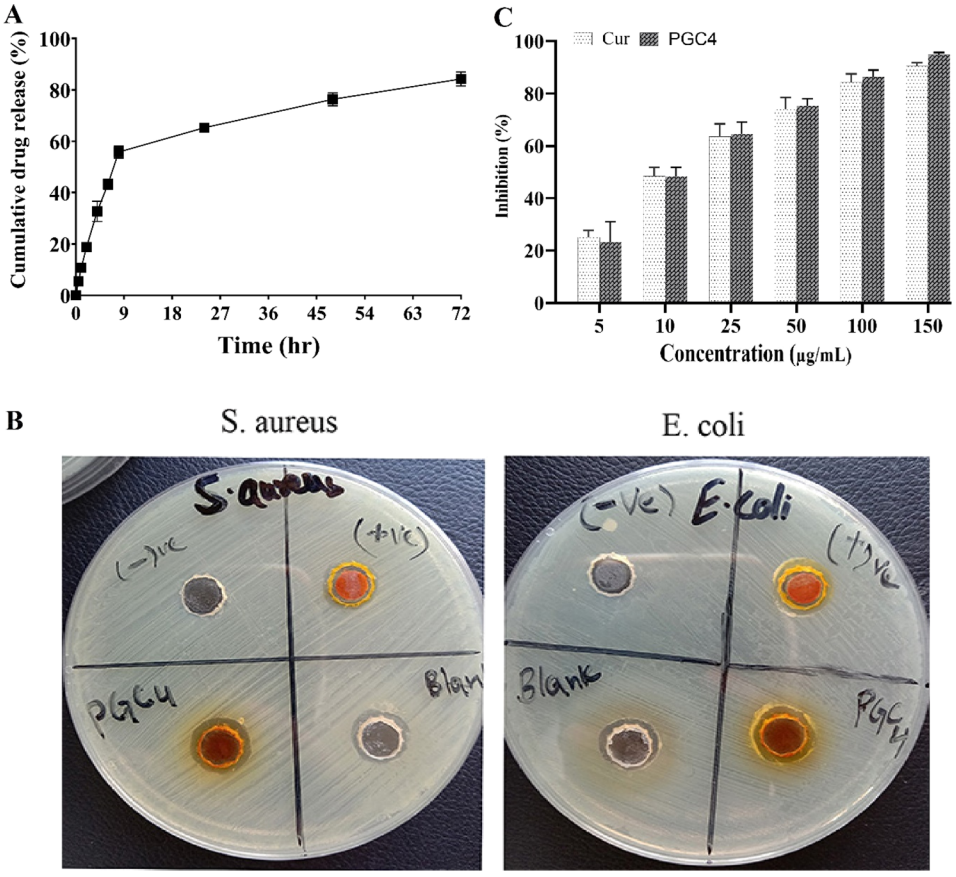

Figure 3. (A) Release behavior of Cur from PGC4 in a mixture of methanol and pH 7.4 PBS (30:70) as release medium. (B) Antibacterial activity of Cur solution (+ve control), PG9 (blank) and PGC4 films against *S. aureus* and *E. coli*. (C) Antioxidant activity of pure Cur and PGC4 in a DPPH scavenging test.

aromatic C—H bonds at 1180 and 767 cm^{-1}, respectively, were also observed.[53,54]

The PG9 exhibited a characteristic band at 3305 cm^{-1} which might be attributed to the phenolic group stretching vibration. The absorption peak that appeared at 2943 cm^{-1} revealed alkane group C—H stretching vibrations. On observing the drug-loaded composite film (PGC4), similar characteristic absorption bands appeared at 3510 cm^{-1}, 1635 cm^{-1}, and 2700 cm^{-1} assigned to OH, NH, and CH groups stretchings, respectively, and the results confirm the Cur compatibility within the film matrix. Hence, the results of FTIR revealed no significant change between drug and polymeric functional groups and also indicated the absence of structural changes in the drug when mixed with polymers. The change in peak intensity was primarily due to the physical interaction among polymers and drug molecules.[36]

3.5.2. X-ray Diffractometry (XRD). XRD highlights the physical state (such as state of crystallinity or amorphous) of samples as depicted in the diffractograms of pure Cur, PG9, and PGC4 in Figure 2D. Pure Cur exhibited crystalline structure with several perceptible sharp diffraction peaks at Bragg's angles (2θ) of 8.61°, 14.34°, 17.05°, 21.03°, 24.38°, 25.46°, and 28.87° which indicated its crystalline nature as mentioned in the literature,[55] while the diffractograms of PG9 and PGC4 came out with no sharp peaks, which divulged the amorphous nature of the drug in the film due to complete drug dispersion in the polymeric matrix.[37,56]

3.5.3. Scanning Electron Microscopy (SEM). SEM images revealed the topography of the blank (PG9) and Cur-loaded composite film (PGC4) as displayed in Figure 2E. Pure Cur showed rod-like morphology or needle shaped crystalline structure as reported elsewhere.[57] The surface of PG9 appeared homogeneous, smooth, nonporous, and compact. The absence of cracks on the film surface has been related to high flexibility.[58] For effective wound dressing, surface integrity is critical, as it hinders entry of infectious microorganisms. The PGC4 surface also did not appear any different from the PG9, thus confirming that the drug was homogeneously dispersed in the film matrix without disturbing the 3D network of the hydrogel film. Moreover, no visual precipitates of the drug were seen, which confirms the results of the XRD as drug remained in the amorphous form even after drying of the films.

3.6. *In-Vitro* Drug Release. Cur release behavior from the composite film was evaluated by a Franz diffusion cell for 72 h in a mixture of buffer (PBS 7.4 pH) and ethanol (70:30 ratio) to meet the sink conditions. Initially, a burst release of about 40% in the first 6 h occurred from the film matrix followed by sustained release over the next 72 h as depicted in Figure 3A. It is reported that free drug molecules might diffuse from the bulk to the surface of the film matrix during the drying process, and then these surface associated molecules give expeditious release when they come into contact with solvent.[59] Moreover, the presence of the surfactant (Tween 80) within the film could also have facilitated the solubilization of the hydrophobic Cur on contact with the release medium. The rapid drug release is most prudent to attain the desired optimal therapeutic effect in the management of wounds followed by a phase of controlled release through the swollen cross-linked polymeric matrix. This

https://doi.org/10.1021/acsomega.2c07018
ACS Omega 2023, 8, 7575−7586

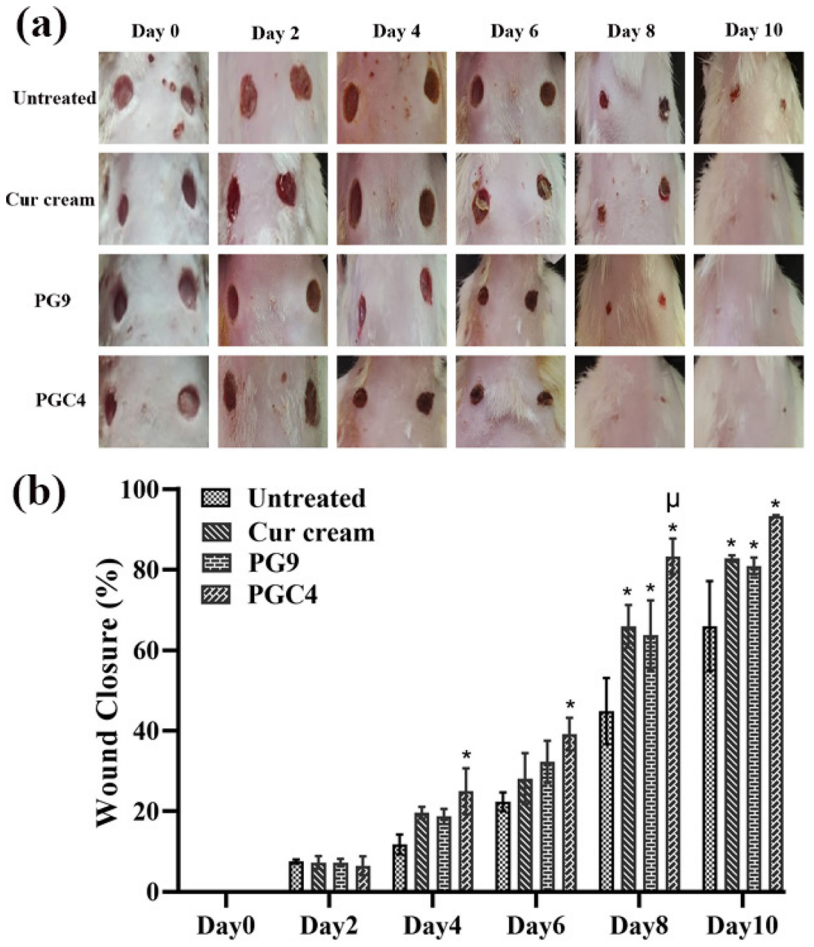

Figure 4. (a) Macroscopic images of wounds treated with different formulations. (b) Graphical illustration of wound closure (n = 3, * indicates significant difference ($p < 0.05$) compared to untreated, μ indicates significant difference ($p < 0.05$) compared to PG9).

sustained release pattern is suitable for maintaining an effective Cur concentration at the wound area to inhibit infection.[32]

To the initial 60% Cur release data form PGC4, the Korsmeyer−Peppas model was applied to understand the release mechanism, and the value of the release parameter, n, was found to be 0.771. $n < 0.45$ is linked to Fickian diffusion, whereas $n > 0.5$ is explained by non-Fickian diffusion, such as drug release that is governed by both diffusion and erosion mechanisms. Hydration of films due to penetration of solvent causes swelling of the polymeric matrix; therefore, drug molecules come out of the film not only due to diffusion but also due to erosion of the swollen polymeric structure.[60,61]

3.7. Biological Evaluation. *3.7.1. Antibacterial Activity.* Effective wound dressings should provide protection against microbes to avoid infection at the wound site and rapid healing.[62] The antibacterial effects of the Cur solution (+ve control), PG9 (blank), and the PGC4 formulation were assessed against both *S. aureus* and *E. coli* as shown in Figure 3B.

Pure Cur (+ve control) exhibited smaller zones of inhibition (12 ± 0.50 mm against *S. aureus* and 10 ± 0.30 against *E. coli*), as the drug's hydrophobicity could have made it difficult to leach into the surrounding nutrient medium.[60] PG9 also showed antimicrobial effects (11.06 ± 0.26 mm against *S. aureus* and 10.16 ± 0.76 against *E. coli*) owing to the presence of TA, but they were weaker than those of the Cur solution and PGC4. Cur and TA could be responsible for the better antimicrobial effect of PGC4 (14.55 ± 0.68 mm against *S. aureus* and 13 ± 1.00 mm against *E. coli*). In addition, the presence of surfactant in the film could also have helped the Cur in penetrating the bacterial cell walls. The increased antimicrobial activity against *S. aureus* compared to *E. coli* might originate from the differences in bacterial cell wall structure of both species, as the complex cell wall of Gram-negative bacteria obstructs the drug entry into the bacteria more efficiently than Gram-positive bacteria.[63] Nonetheless, PGC4 could be used as an effective material for wounds not only by restricting access of the microbes to the wound bed but also due to its ability to kill them.

3.7.2. Antioxidant Assay. Cur is well-known for its antioxidant activity against reactive oxygen species (ROS). The percentage ROS inhibition of Cur and PGC4 was evaluated (Figure 3C) by investigating their capability to scavenge DPPH free radical by e^- transfer or H atom donation from the polyphenolic −OH group of Cur and TA that alter the stable DPPH into its reduced form.[53]

The percent ROS inhibition activities of pure drug and PGC4 gradually increased with increase in Cur concentration. At higher Cur concentration, PGC4 demonstrated slightly better but statistically insignificant ($p > 0.05$) antioxidant activity which could be linked to the presence of TA. Henceforth, PGC4 retained the antioxidant potential of Cur after its incorporation in the polymeric matrix, and it could prevent the ROS at the wound site that impedes the healing process.

https://doi.org/10.1021/acsomega.2c07018
ACS Omega 2023, 8, 7575−7586

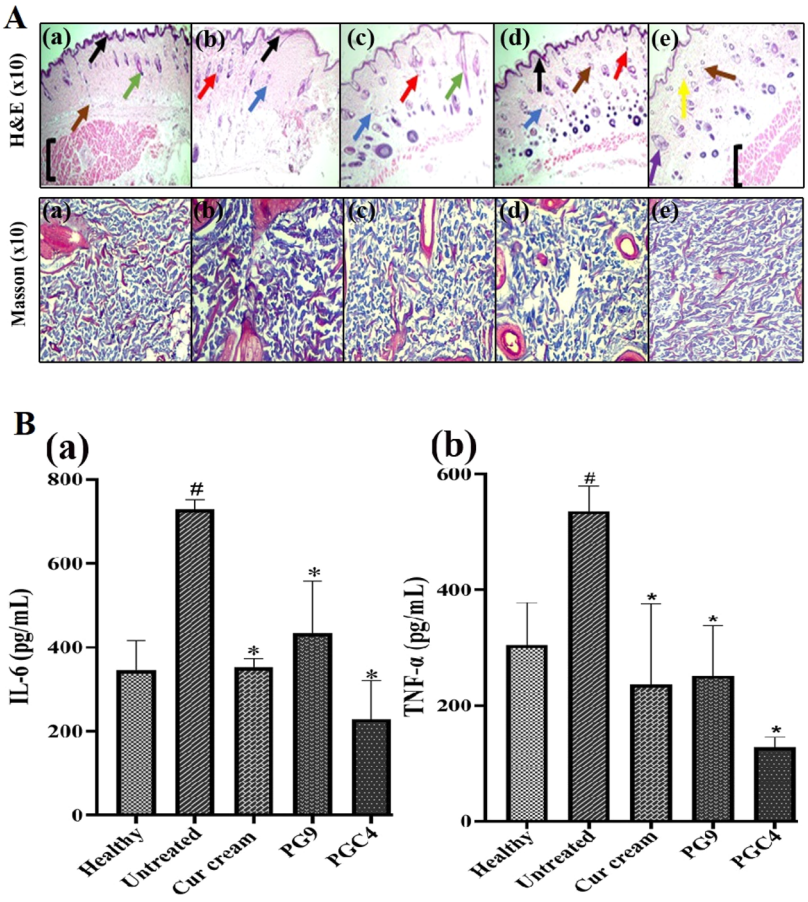

Figure 5. (A) H&E and Masson trichrome staining of healed incisions (microscopic views) at the 10th day of post-wounding in different experimental groups: (a) healthy; (b) untreated; (c) Cur cream; (d) PG9; (e) PGC4. Black arrows show epidermis, red for neutrophil, dark brown for blood vessels, green for hair follicles, blue for inflammatory cells, yellow for collagen, purple for sebaceous gland, and black brackets indicate connective tissue. (B) Expression of (a) IL-6 and (b) TNF-α levels (n = 3). # indicates significant difference ($p < 0.05$) compared to healthy, * indicates significant difference ($p < 0.05$) compared to untreated group.

3.7.3. In-Vivo Wound Healing Study. Full thickness wounds were created in albino rats to evaluate the percentage wound closure of PGC4 and compare it with PG9 and Cur cream. The visual observations of wounds at different time intervals presented that wound area reduced in a time-dependent manner in all groups, while it was more prominent for animals treated with PGC4. The results of wound contraction are shown in Figure 4(a). The statistical analysis indicated that the time and types of treatments had significant effects on wound closure ($p < 0.05$). On the fourth day, significant wound contraction was observed in animals treated with the PGC4 formulation, compared to animals receiving no treatment. Cur cream and PG9 also exhibited superior wound closure compared to untreated on the eighth and 10th days as shown in Figure 4(b). On the 10th day, complete wound closure (93%) was observed only in the PGC4 group. Cur cream and PG9 showed almost identical wound closure, but the results of PGC4 were comparatively better than those of all other groups. These results indicate that the Cur-loaded film maintained an environment that promoted wound closure due to appropriate antioxidant, anti-inflammatory and antibacterial coverage of Cur.

3.7.4. Histopathological Examination. At the 10th day (final time point) of *in-vivo* animal study, skin wound samples were harvested, and histopathological examination was executed using H&E and Masson's trichrome stains to further assess the skin layers, angiogenesis, and deposition of collagen[64] as shown in Figure 5A. Rats treated with the PGC4 formulation showed epidermal proliferation, whereas the skin structure of the wound tissue was similar to healthy skin with a regular epidermal structure, several instances of neovascularization, and numerous granulation tissue formations, which were more prominent in comparison to other experimental groups. Moreover, a decreased number of inflammatory cells were also observed in the PGC4 group due to the potential scavenging of free oxygen radicals. Furthermore, better rejuvenation of skin was further improved by gelatin and TA in composite films, thus accelerating the wound healing process.[33]

As shown in Figure 5A(a), the uniform arrangement of collagen fibers and the amount of collagen revealed the degree of wound healing in the Masson's trichome staining. Collagen was stained blue while keratin and muscle fibers were stained red. The intensity of color resembled the amount of collagen deposition followed by development of collagen synthesis and remodeling.[18] The collagen fibers in the PGC4 group were organized in a uniform manner, and their morphology was very close to that of normal healthy skin. The PG9 group also exhibited collagen deposition with an irregular pattern that might be due to the high content of gelatin in the composite film. Similarly, the group treated with Cur cream also showed an irregular pattern of collagen formation, whereas deceased

https://doi.org/10.1021/acsomega.2c07018
ACS Omega 2023, 8, 7575−7586

collagen production was observed in the untreated control group.[65] As the collagen is made from fibroblasts, so an increase in collagen amount reveals a rise in fibroblast formation;[66] hence, it was also demonstrated in our study that Cur-loaded PGC4 influenced fibroblast proliferation to accelerate the healing process. The histological data evidently specify that our composite films accelerated and enhanced the more natural way of tissue rejuvenation in the full thickness excisional rat wound model.

3.7.5. Inflammatory Biomarkers. In the acute inflammatory phase of the normal healing process, several chemokines, cytokines, and growth factors are secreted. Persistent inflammation is responsible for the increased release of IL-6 and TNF-α. The overexpression of IL-6 and TNF-α retard the contraction of wounds and exacerbate other skin pathological conditions; therefore, controlling these mediators could expedite the healing process of wounds.[67] Higher levels of these inflammatory biomarkers were also observed in the untreated group in our study. All the treatment groups showed marked lowering of the elevated inflammatory mediators. Figure 5B shows the levels of the inflammatory mediators in rats' plasma at the end of the study. The *in-vivo* anti-inflammatory effect of Cur at the wound site was demonstrated by lowering of the TNF-α and IL-6 levels as observed elsewhere.[68] Mohanty and Pradhan reported the down-regulation of pro-inflammatory cytokines by Cur-loaded polymeric bandages.[69] The equivalent performance of the PG9 indicated that the blank film worked as an excellent dressing material by maintaining the environment conducive for the healing of the wounds. Expression of TNF-α and IL-6 decreased significantly in the rats treated with PGC4 when compared to untreated groups. Although PGC4 yielded results that did not differ statistically from those of other treatment groups but the decline in TNF-α and IL-6 levels was more prominent, that is why, early and almost fully healed wounds were recorded in the rats treated with PGC4. We can infer that PGC4 exploited the maximum therapeutic potential of the Cur in the wound healing process.

4. CONCLUSION

In summary, we successfully prepared a bioactive wound dressing film (PGC4) based on cross-linking of PVA/gelatin composites via TA for encapsulation of Cur to promote the healing process. Physicochemical, mechanical and solid-state characterization revealed the suitability of the biocomposite film as a wound dressing by offering sufficient mechanical strength and capability to maintain the moist environment at the wound site by absorbing wound exudates. Cur loading in the film promoted its *in-vitro* antibacterial and antioxidant potential because of the prolonged release of drug. More importantly, an *in-vivo* wound healing study in the full thickness wound model in rats presented accelerated epidermal regeneration, faster collagen deposition, and more pronounced lowering of the inflammatory cytokines by the PGC4. Hence, the PGC4 composite film developed in the current work displayed encouraging results, and it holds potential as an effective bioactive wound dressing that should be further established through enzymatic cytotoxicity assays and immunostaining studies.

ASSOCIATED CONTENT

Supporting Information

The Supporting Information is available free of charge at https://pubs.acs.org/doi/10.1021/acsomega.2c07018.

Swelling indexes of composite films. (PDF)

AUTHOR INFORMATION

Corresponding Author

Sajid Asghar − *Department of Pharmaceutics, Faculty of Pharmaceutical Sciences, Government College University Faisalabad, Faisalabad 38000, Pakistan*; orcid.org/0000-0002-9184-9098; Email: sajidasghar@gcuf.edu.pk, sajuhappa@gmail.com

Authors

Nida Rashid − *Department of Pharmaceutics, Faculty of Pharmaceutical Sciences, Government College University Faisalabad, Faisalabad 38000, Pakistan*

Syed Haroon Khalid − *Department of Pharmaceutics, Faculty of Pharmaceutical Sciences, Government College University Faisalabad, Faisalabad 38000, Pakistan*

Ikram Ullah Khan − *Department of Pharmaceutics, Faculty of Pharmaceutical Sciences, Government College University Faisalabad, Faisalabad 38000, Pakistan*

Zunera Chauhdary − *Department of Pharmacology, Faculty of Pharmaceutical Sciences, Government College University Faisalabad, Faisalabad 38000, Pakistan*

Hira Mahmood − *Department of Pharmaceutics, Faculty of Pharmaceutical Sciences, Government College University Faisalabad, Faisalabad 38000, Pakistan*

Ayesha Saleem − *Department of Pharmaceutics, Faculty of Pharmaceutical Sciences, Government College University Faisalabad, Faisalabad 38000, Pakistan*

Muhammad Umair − *Department of Pharmaceutics, Faculty of Pharmaceutical Sciences, Government College University Faisalabad, Faisalabad 38000, Pakistan*

Complete contact information is available at: https://pubs.acs.org/10.1021/acsomega.2c07018

Funding

This research received no external funding.

Notes

The authors declare no competing financial interest.

ACKNOWLEDGMENTS

The authors acknowledge the Department of Pharmaceutics, Faculty of Pharmaceutical Sciences, Government College University Faisalabad, for providing the necessary support and facilities for the completion of the project.

REFERENCES

(1) Kamoun, E. A.; Kenawy, E.-R. S.; Chen, X. A review on polymeric hydrogel membranes for wound dressing applications: PVA-based hydrogel dressings. *J. Adv. Res.* **2017**, *8* (3), 217−233. Moeini, A.; Pedram, P.; Makvandi, P.; Malinconico, M.; Gomez d'Ayala, G. Wound healing and antimicrobial effect of active secondary metabolites in chitosan-based wound dressings: a review. *Carbohydr. Polym.* **2020**, *233*, 115839.

(2) Rodríguez-Rodríguez, R.; Espinosa-Andrews, H.; Velasquillo-Martínez, C.; García-Carvajal, Z. Y. Composite hydrogels based on gelatin, chitosan and polyvinyl alcohol to biomedical applications: a review. *Int. J. Polym. Mater. Polym. Biomater.* **2020**, *69* (1), 1−20.

(3) Moura, L. I.; Dias, A. M.; Carvalho, E.; de Sousa, H. C. Recent advances on the development of wound dressings for diabetic foot ulcer treatment—A review. *Acta Biomater.* **2013**, *9* (7), 7093−7114.
(4) Zhang, S.; Li, J.; Chen, S.; Zhang, X.; Ma, J.; He, J. Oxidized cellulose-based hemostatic materials. *Carbohydr. Polym.* **2020**, *230*, 115585.
(5) Tao, G.; Wang, Y.; Cai, R.; Chang, H.; Song, K.; Zuo, H.; Zhao, P.; Xia, Q.; He, H. Design and performance of sericin/poly (vinyl alcohol) hydrogel as a drug delivery carrier for potential wound dressing application. *Mater. Sci. Eng., C* **2019**, *101*, 341−351.
(6) Fan, L.; Yang, H.; Yang, J.; Peng, M.; Hu, J. Preparation and characterization of chitosan/gelatin/PVA hydrogel for wound dressings. *Carbohydr. Polym.* **2016**, *146*, 427−434.
(7) Karthika, A.; Kavitha, L.; Surendiran, M.; Kannan, S.; Gopi, D. Fabrication of divalent ion substituted hydroxyapatite/gelatin nanocomposite coating on electron beam treated titanium: mechanical, anticorrosive, antibacterial and bioactive evaluations. *RSC Adv.* **2015**, *5* (59), 47341−47352.
(8) Sakthiguru, N.; Sithique, M. A. Fabrication of bioinspired chitosan/gelatin/allantoin biocomposite film for wound dressing application. *Int. J. Biol. Macromol.* **2020**, *152*, 873−883.
(9) Shah, S. A.; Sohail, M.; Khan, S.; Minhas, M. U.; De Matas, M.; Sikstone, V.; Hussain, Z.; Abbasi, M.; Kousar, M. Biopolymer-based biomaterials for accelerated diabetic wound healing: A critical review. *Int. J. Biol. Macromol.* **2019**, *139*, 975−993.
(10) Gelli, R.; Del Buffa, S.; Tempesti, P.; Bonini, M.; Ridi, F.; Baglioni, P. Multi-scale investigation of gelatin/poly (vinyl alcohol) interactions in water. *Colloids Surf. Physicochem. Eng. Aspects* **2017**, *532*, 18−25.
(11) Feki, A.; Bardaa, S.; Hajji, S.; Ktari, N.; Hamdi, M.; Chabchoub, N.; Kallel, R.; Boudawara, T.; Nasri, M.; Ben Amara, I. Falkenbergia rufolanosa polysaccharide-Poly (vinyl alcohol) composite films: A promising wound healing agent against dermal laser burns in rats. *Int. J. Biol. Macromol.* **2020**, *144*, 954−966. Adeli, H.; Khorasani, M. T.; Parvazinia, M. Wound dressing based on electrospun PVA/chitosan/starch nanofibrous mats: Fabrication, antibacterial and cytocompatibility evaluation and in vitro healing assay. *Int. J. Biol. Macromol.* **2019**, *122*, 238−254.
(12) Badawy, S. M. Green synthesis and characterisations of antibacterial silver-polyvinyl alcohol nanocomposite films for wound dressing. *Green Processing and Synthesis* **2014**, *3* (3), 229−234.
(13) Sharma, S.; Tiwari, S. A review on biomacromolecular hydrogel classification and its applications. *Int. J. Biol. Macromol.* **2020**, *162*, 737−747.
(14) Xu, F.; Weng, B.; Gilkerson, R.; Materon, L. A.; Lozano, K. Development of tannic acid/chitosan/pullulan composite nanofibers from aqueous solution for potential applications as wound dressing. *Carbohydr. Polym.* **2015**, *115*, 16−24.
(15) Aewsiri, T.; Benjakul, S.; Visessanguan, W.; Wierenga, P. A.; Gruppen, H. Antioxidative activity and emulsifying properties of cuttlefish skin gelatin-tannic acid complex as influenced by types of interaction. *Innovative Food Sci. Emerging Technol.* **2010**, *11* (4), 712−720.
(16) Taheri, P.; Jahanmardi, R.; Koosha, M.; Abdi, S. Physical, mechanical and wound healing properties of chitosan/gelatin blend films containing tannic acid and/or bacterial nanocellulose. *Int. J. Biol. Macromol.* **2020**, *154*, 421−432.
(17) Ari, B.; Sahiner, M.; Demirci, S.; Sahiner, N. Poly (vinyl alcohol)-tannic acid cryogel matrix as antioxidant and antibacterial material. *Polymers* **2022**, *14* (1), 70.
(18) Zahiri, M.; Khanmohammadi, M.; Goodarzi, A.; Ababzadeh, S.; Sagharjoghi Farahani, M.; Mohandesnezhad, S.; Bahrami, N.; Nabipour, I.; Ai, J. Encapsulation of curcumin loaded chitosan nanoparticle within poly (ε-caprolactone) and gelatin fiber mat for wound healing and layered dermal reconstitution. *Int. J. Biol. Macromol.* **2020**, *153*, 1241−1250.
(19) Khamrai, M.; Banerjee, S. L.; Paul, S.; Samanta, S.; Kundu, P. P. Curcumin entrapped gelatin/ionically modified bacterial cellulose based self-healable hydrogel film: An eco-friendly sustainable synthesis method of wound healing patch. *Int. J. Biol. Macromol.* **2019**, *122*, 940−953.
(20) Chiaoprakobkij, N.; Suwanmajo, T.; Sanchavanakit, N.; Phisalaphong, M. Curcumin-loaded bacterial cellulose/alginate/gelatin as a multifunctional biopolymer composite film. *Molecules* **2020**, *25* (17), 3800.
(21) Roy, S.; Rhim, J.-W. Carboxymethyl cellulose-based antioxidant and antimicrobial active packaging film incorporated with curcumin and zinc oxide. *Int. J. Biol. Macromol.* **2020**, *148*, 666−676.
(22) Patel, S.; Srivastava, S.; Singh, M. R.; Singh, D. Preparation and optimization of chitosan-gelatin films for sustained delivery of lupeol for wound healing. *Int. J. Biol. Macromol.* **2018**, *107*, 1888−1897.
(23) Limpongsa, E.; Soe, M. T.; Jaipakdee, N. Modification of release and penetration behavior of water-soluble active ingredient from ball-milled glutinous starch matrix via carboxymethylcellulose blending. *Int. J. Biol. Macromol.* **2021**, *193*, 2271−2280.
(24) Thakur, G.; Singh, A.; Singh, I. Formulation and evaluation of transdermal composite films of chitosan-montmorillonite for the delivery of curcumin. *Int. J. Pharm. Invest.* **2016**, *6* (1), 23.
(25) Wang, P.; Li, Y.; Zhang, C.; Que, F.; Weiss, J.; Zhang, H. Characterization and antioxidant activity of trilayer gelatin/dextran-propyl gallate/gelatin films: Electrospinning versus solvent casting. *Lwt* **2020**, *128*, 109536.
(26) Orsuwan, A.; Shankar, S.; Wang, L.-F.; Sothornvit, R.; Rhim, J.-W. Preparation of antimicrobial agar/banana powder blend films reinforced with silver nanoparticles. *Food Hydrocolloids* **2016**, *60*, 476−485.
(27) Singh, S.; Nwabor, O. F.; Syukri, D. M.; Voravuthikunchai, S. P. Chitosan-poly (vinyl alcohol) intelligent films fortified with anthocyanins isolated from Clitoria ternatea and Carissa carandas for monitoring beverage freshness. *Int. J. Biol. Macromol.* **2021**, *182*, 1015−1025.
(28) Luo, R.; Lin, M.; Zhang, C.; Shi, J.; Zhang, S.; Chen, Q.; Hu, Y.; Zhang, M.; Zhang, J.; Gao, F. Genipin-crosslinked human serum albumin coating using a tannic acid layer for enhanced oral administration of curcumin in the treatment of ulcerative colitis. *Food Chem.* **2020**, *330*, 127241.
(29) Miskeen, S.; An, Y. S.; Kim, J.-Y. Application of starch nanoparticles as host materials for encapsulation of curcumin: Effect of citric acid modification. *Int. J. Biol. Macromol.* **2021**, *183*, 1−11.
(30) Ni, Y.; Nie, H.; Wang, J.; Lin, J.; Wang, Q.; Sun, J.; Zhang, W.; Wang, J. Enhanced functional properties of chitosan films incorporated with curcumin-loaded hollow graphitic carbon nitride nanoparticles for bananas preservation. *Food Chem.* **2022**, *366*, 130539.
(31) Chin, C.-Y.; Jalil, J.; Ng, P. Y.; Ng, S.-F. Development and formulation of Moringa oleifera standardised leaf extract film dressing for wound healing application. *J. Ethnopharmacol.* **2018**, *212*, 188−199.
(32) Zainuddin, N.; Ahmad, I.; Zulfakar, M. H.; Kargarzadeh, H.; Ramli, S. Cetyltrimethylammonium bromide-nanocrystalline cellulose (CTAB-NCC) based microemulsions for enhancement of topical delivery of curcumin. *Carbohydr. Polym.* **2021**, *254*, 117401.
(33) Chen, K.; Pan, H.; Ji, D.; Li, Y.; Duan, H.; Pan, W. Curcumin-loaded sandwich-like nanofibrous membrane prepared by electrospinning technology as wound dressing for accelerate wound healing. *Mater. Sci. Eng., C* **2021**, *127*, 112245.
(34) Ashraf, U.; Khan, S.-U.-D.; Asghar, S.; IRFAN, M.; Khan, I. U.; Shah, P. A.; Saleem, M.; Rasul, A.; Imran, K.; Bashir, R.; et al. Development and Validation of a RP-HPLC Method for Determination of Chondroitin Sulphate and Curcumin in Topical Formulation. *Lat. Am. J. Pharm.* **2021**, *40* (10), 2346−2354.
(35) Alqahtani, M. S.; Alqahtani, A.; Kazi, M.; Ahmad, M. Z.; Alahmari, A.; Alsenaidy, M. A.; Syed, R. Wound-healing potential of curcumin loaded lignin nanoparticles. *J. Drug Delivery Sci. Technol.* **2020**, *60*, 102020.
(36) Roy, S.; Rhim, J.-W. Preparation of antimicrobial and antioxidant gelatin/curcumin composite films for active food packaging application. *Colloids Surf. B. Biointerfaces* **2020**, *188*, 110761.

https://doi.org/10.1021/acsomega.2c07018
ACS Omega 2023, 8, 7575−7586

(37) Liu, Y.; Cai, Y.; Jiang, X.; Wu, J.; Le, X. Molecular interactions, characterization and antimicrobial activity of curcumin-chitosan blend films. *Food Hydrocolloids* **2016**, *52*, 564−572.
(38) Ng, S.-F.; Jumaat, N. Carboxymethyl cellulose wafers containing antimicrobials: a modern drug delivery system for wound infections. *Eur. J. Pharm. Sci.* **2014**, *51*, 173−179.
(39) Satish, A.; Aswathi, R.; Caroline Maria, J.; Sai Korrapati, P. Triiodothyronine impregnated alginate/gelatin/polyvinyl alcohol composite scaffold designed for exudate-intensive wound therapy. *Eur. Polym. J.* **2019**, *110*, 252−264.
(40) Sahiner, N.; Sagbas, S.; Sahiner, M.; Silan, C.; Aktas, N.; Turk, M. Biocompatible and biodegradable poly (Tannic Acid) hydrogel with antimicrobial and antioxidant properties. *Int. J. Biol. Macromol.* **2016**, *82*, 150−159.
(41) Ghaderi, J.; Hosseini, S. F.; Keyvani, N.; Gómez-Guillén, M. C. Polymer blending effects on the physicochemical and structural features of the chitosan/poly (vinyl alcohol)/fish gelatin ternary biodegradable films. *Food Hydrocolloids* **2019**, *95*, 122−132.
(42) Pal, K.; Banthia, A.; Majumdar, D. Biomedical evaluation of polyvinyl alcohol-gelatin esterified hydrogel for wound dressing. *J. Mater. Sci. Mater. Med.* **2007**, *18* (9), 1889−1894.
(43) Chambi, H.; Grosso, C. Edible films produced with gelatin and casein cross-linked with transglutaminase. *Food Res. Int.* **2006**, *39* (4), 458−466.
(44) Acosta, S.; Chiralt, A.; Santamarina, P.; Rosello, J.; González-Martínez, C.; Cháfer, M. Antifungal films based on starch-gelatin blend, containing essential oils. *Food hydrocolloids* **2016**, *61*, 233−240.
(45) Musso, Y. S.; Salgado, P. R.; Mauri, A. N. Smart edible films based on gelatin and curcumin. *Food hydrocolloids* **2017**, *66*, 8−15.
(46) Núñez-Flores, R.; Giménez, B.; Fernández-Martín, F.; López-Caballero, M.; Montero, M.; Gómez-Guillén, M. Physical and functional characterization of active fish gelatin films incorporated with lignin. *Food Hydrocolloids* **2013**, *30* (1), 163−172.
(47) Pellá, M. C.; Silva, O. A.; Pellá, M. G.; Beneton, A. G.; Caetano, J.; Simões, M. R.; Dragunski, D. C. Effect of gelatin and casein additions on starch edible biodegradable films for fruit surface coating. *Food Chem.* **2020**, *309*, 125764.
(48) Wang, L.; Xue, J.; Zhang, Y. Preparation and characterization of curcumin loaded caseinate/zein nanocomposite film using pH-driven method. *Ind. Crops Prod.* **2019**, *130*, 71−80.
(49) Dammak, I.; Lourenco, R. V.; do Amaral Sobral, P. J. Active gelatin films incorporated with Pickering emulsions encapsulating hesperidin: Preparation and physicochemical characterization. *J. Food Eng.* **2019**, *240*, 9−20.
(50) Yang, X.; Chen, M.; Li, P.; Ji, Z.; Wang, M.; Feng, Y.; Shi, C. Fabricating poly (vinyl alcohol)/gelatin composite sponge with high absorbent and water-triggered expansion for noncompressible hemorrhage and wound healing. *J. Mater. Chem. B* **2021**, *9*, 1568−1582.
(51) Roy, S.; Rhim, J.-W. Preparation of bioactive functional poly (lactic acid)/curcumin composite film for food packaging application. *Int. J. Biol. Macromol.* **2020**, *162*, 1780−1789.
(52) Zhang, Z.-Y.; Sun, Y.; Zheng, Y.-D.; He, W.; Yang, Y.-Y.; Xie, Y.-J.; Feng, Z.-X.; Qiao, K. A biocompatible bacterial cellulose/tannic acid composite with antibacterial and anti-biofilm activities for biomedical applications. *Mater. Sci. Eng., C* **2020**, *106*, 110249.
(53) Ulu, A.; Birhanli, E.; Ateş, B. Tunable and tough porous chitosan/β-cyclodextrin/tannic acid biocomposite membrane with mechanic, antioxidant, and antimicrobial properties. *Int. J. Biol. Macromol.* **2021**, *188*, 696−707.
(54) Halim, A. L. A.; Kamari, A.; Phillip, E. Chitosan, gelatin and methylcellulose films incorporated with tannic acid for food packaging. *Int. J. Biol. Macromol.* **2018**, *120*, 1119−1126.
(55) Hussein, Y.; Loutfy, S. A.; Kamoun, E. A.; El-Moslamy, S. H.; Radwan, E. M.; Elbehairi, S. E. I. Enhanced anti-cancer activity by localized delivery of curcumin form PVA/CNCs hydrogel membranes: preparation and in vitro bioevaluation. *Int. J. Biol. Macromol.* **2021**, *170*, 107−122.
(56) Chauhan, S.; Bansal, M.; Khan, G.; Yadav, S. K.; Singh, A. K.; Prakash, P.; Mishra, B. Development, optimization and evaluation of curcumin loaded biodegradable crosslinked gelatin film for the effective treatment of periodontitis. *Drug Dev. Ind. Pharm.* **2018**, *44* (7), 1212−1221.
(57) Venkatasubbu, G. D.; Anusuya, T. Investigation on Curcumin nanocomposite for wound dressing. *Int. J. Biol. Macromol.* **2017**, *98*, 366−378.
(58) Dafader, N. C.; Rahman, S. T.; Rahman, W.; Rahman, N.; Manir, M.; Alam, M.; Alam, J.; Sumi, S. A. Preparation of gelatin/poly (vinyl alcohol) film modified by methyl methacrylate and gamma irradiation. *Int. J. Polym. Anal. Charact.* **2016**, *21* (6), 513−523.
(59) Ghorpade, V. S.; Yadav, A. V.; Dias, R. J.; Mali, K. K.; Pargaonkar, S. S.; Shinde, P. V.; Dhane, N. S. Citric acid crosslinked carboxymethylcellulose-poly (ethylene glycol) hydrogel films for delivery of poorly soluble drugs. *Int. J. Biol. Macromol.* **2018**, *118*, 783−791.
(60) Tummalapalli, M.; Berthet, M.; Verrier, B.; Deopura, B.; Alam, M.; Gupta, B. Composite wound dressings of pectin and gelatin with aloe vera and curcumin as bioactive agents. *Int. J. Biol. Macromol.* **2016**, *82*, 104−113.
(61) Tampau, A.; González-Martínez, C.; Chiralt, A. Release kinetics and antimicrobial properties of carvacrol encapsulated in electrospun poly-(ϵ-caprolactone) nanofibres. Application in starch multilayer films. *Food Hydrocolloids* **2018**, *79*, 158−169.
(62) Manna, P. J.; Mitra, T.; Pramanik, N.; Kavitha, V.; Gnanamani, A.; Kundu, P. Potential use of curcumin loaded carboxymethylated guar gum grafted gelatin film for biomedical applications. *Int. J. Biol. Macromol.* **2015**, *75*, 437−446.
(63) Asghar, S.; Khan, I. U.; Salman, S.; Khalid, S. H.; Ashfaq, R.; Vandamme, T. F. Plant-derived nanotherapeutic systems to counter the overgrowing threat of resistant microbes and biofilms. *Adv. Drug Delivery Rev.* **2021**, *179*, 114019.
(64) Liao, H. T.; Lai, Y.-T.; Kuo, C.-Y.; Chen, J.-P. A bioactive multi-functional heparin-grafted aligned poly (lactide-co-glycolide)/curcumin nanofiber membrane to accelerate diabetic wound healing. *Mater. Sci. Eng., C* **2021**, *120*, 111689.
(65) Guo, R.; Lan, Y.; Xue, W.; Cheng, B.; Zhang, Y.; Wang, C.; Ramakrishna, S. Collagen-cellulose nanocrystal scaffolds containing curcumin-loaded microspheres on infected full-thickness burns repair. *J. Tissue Eng. Regen. Med.* **2017**, *11* (12), 3544−3555.
(66) Zhang, J.; Ding, C.; Yue, Z.; Sun, S.; Zheng, Y.; Ding, Q.; Hong, B.; Liu, W. Fabrication of chitosan/PVP/dihydroquercetin nanocomposite film for in vitro and in vivo evaluation of wound healing. *Int. J. Biol. Macromol.* **2022**, *206*, 591−604.
(67) Wetzler, C.; Kämpfer, H.; Stallmeyer, B.; Pfeilschifter, J.; Frank, S. Large and sustained induction of chemokines during impaired wound healing in the genetically diabetic mouse: prolonged persistence of neutrophils and macrophages during the late phase of repair. *J. Invest. Dermatol.* **2000**, *115* (2), 245−253.
(68) Kant, V.; Gopal, A.; Pathak, N. N.; Kumar, P.; Tandan, S. K.; Kumar, D. Antioxidant and anti-inflammatory potential of curcumin accelerated the cutaneous wound healing in streptozotocin-induced diabetic rats. *Int. Immunopharmacol.* **2014**, *20* (2), 322−330.
(69) Mohanty, C.; Pradhan, J. A human epidermal growth factor-curcumin bandage bioconjugate loaded with mesenchymal stem cell for in vivo diabetic wound healing. *Mater. Sci. Eng., C* **2020**, *111*, 110751.

https://doi.org/10.1021/acsomega.2c07018
ACS Omega 2023, 8, 7575−7586